INTERNATIONAL JOURNAL OF CLIMATOLOGY
Int. J. Climatol. **26**: 1001–1016 (2006)
Published online 20 February 2006 in Wiley InterScience (www.interscience.wiley.com). DOI: 10.1002/joc.1300

SYNOPTIC CLIMATOLOGY OF EXTREME FIRE-WEATHER CONDITIONS ACROSS THE SOUTHWEST UNITED STATES

MICHAEL A. CRIMMINS*
Department of Soil, Water & Environmental Science, The University of Arizona, Tucson, Arizona 85721-0038, USA

Received 29 January 2005
Revised 4 October 2005
Accepted 11 November 2005

ABSTRACT

Extreme fire-weather conditions are usually thought of as discrete events rather than part of a continuum of meteorological and climatological variability. This study uses a synoptic climatological approach (weather typing) to examine the seasonal climatology of extreme fire-weather conditions across the southwest United States (Arizona and New Mexico) during the period of 1988–2003. Three key circulation patterns representing broad southwesterly flow and large geopotential height gradients are associated with over 80% of the extreme fire-weather days identified in this study. Seasonal changes in relative humidity levels, strength of height gradient, and geopotential heights all modulate the relationship between these key circulation patterns and extreme fire-weather days. Examination of daily incident summaries for three recent wildfires (May 2000, June 2002 and June 2003) shows that wildfire activity can be strongly regulated by these critical fire-weather circulation patterns. Copyright © 2006 Royal Meteorological Society.

KEY WORDS: fire weather; synoptic weather types; self-organizing maps; wildfires; southwest United States

1. INTRODUCTION

The importance of weather conditions to the behavior and rate of spread of a wildfire is well documented (Flannigan and Harrington, 1988; Bessie and Johnson, 1995; Burgan *et al*., 1997; Flannigan and Wotton, 2001). Studies of the interaction between fire-weather conditions and wildfire activity have focused on modeling short timescale meteorologic and wildfire behavior variability (Fujioka, 1997; Andrews and Queen, 2001). Modeling efforts have helped quantify the role of weather variability relative to fuel conditions and amounts and local topography (Deeming *et al*., 1977; Burgan, 1988; Pyne *et al*., 1996). The development of fire danger rating systems has allowed for the integration of longer-term (seasonal) climatic variability and short-term meteorological variability into decision support tools for fire management. Seasonal changes (drying or wetting) of fuels can be tracked with metrics like the energy release component (ERC) and integrated with daily weather indices, such as the spread component (SC), both components of the US National Fire Danger Rating System (NFDRS), to evaluate daily fire danger.

The integration of cumulative indices (e.g. ERC) that represent seasonal climatological changes with daily fire-weather variability represent only part of the temporal range important in controlling interannual wildfire activity. The role of low-frequency climatic variability in controlling seasonal wildfire activity, especially in the southwest United States, represents a newly discovered dimension of wildfire climatology. Recent studies in the southwest United States have found that antecedent conditions (i.e. years prior to wildfire seasons) can influence overall wildfire activity through precipitation either limiting or promoting the growth of fine fuels and through direct control of fuel moisture levels (Swetnam and Betancourt, 1990, 1998; Westerling *et al*., 2002, 2003; Crimmins and Comrie, 2004). Southwestern wildfire regimes respond to both short-term and

* Correspondence to: Michael A. Crimmins, Department of Soil, Water & Environmental Science, The University of Arizona, Tucson, Arizona 85721-0038, USA; e-mail: crimmins@u.arizona.edu

long-term atmospheric variability through precipitation-fuel production mechanisms, seasonal and interannual drought conditions, and daily fluctuations in relative humidity, wind speeds, and temperature. All of these components are inextricably linked to synoptic-scale circulation patterns, which can provide diagnostics of both high- and low-frequency variability within the context of a global system. Examining the connection between synoptic circulation patterns and surface fire-weather conditions is a crucial component in attempting to construct a more complete understanding of the interactions between wildfire and climate variability across the southwestern United States.

Schroeder (1969) recognized that linking large-scale synoptic patterns with regional- to local-scale fire danger was an effective way of constructing a fire-weather climatology for the conterminous United States. He developed daily fire danger ratings for several regions across the United States and then evaluated the dominant synoptic circulation patterns that occurred on days with extreme ratings. His study, published over 30 years ago, is arguably the most utilized example of a fire-weather climatology. It is an integral part of training fire managers and fire suppression personnel in basic fire-weather concepts. Several studies have analyzed the synoptic circulation patterns associated with wildfire events (Brotak and Reifsnyder, 1977; Johnson and Wowchuk, 1993; Takle *et al*., 1994), but few have employed a synoptic climatological approach to examine daily fire-weather variability. The Schroeder (1969) study used daily weather data for the period of 1951–1960, which has not been reevaluated with more contemporary data to examine the stability of the findings.

The objective of this study is to relate daily surface fire-weather index values to their respective synoptic circulation patterns and to characterize the environmental conditions within the key patterns. Through this objective, an evaluation of the utility of automatic synoptic classification systems with respect to fire weather will be gained. The study focuses on determining the synoptic weather patterns associated with elevated fire danger across the southwest United States and examines the circulation patterns associated with a three-case study of wildfire events. The seasonal continuum of synoptic types is considered to determine whether seasonal changes in extreme fire-weather conditions are associated with changes in circulation patterns. This detailed examination of critical fire-weather circulation patterns will be useful in further diagnostic studies linking low-frequency climate variability and variability in regional fire weather.

2. DATA AND METHODS

2.1. Synoptic circulation classification

Daily synoptic-scale circulation patterns were classified into different key weather types using an unsupervised classification technique known as the *self-organizing map* (SOM) algorithm (Kohonen, 2001). It is essentially a nonlinear, iterative clustering algorithm. This technique has been utilized in many different disciplines for several years, but has only recently seen wider utilization within the field of climatology (Cavazos, 2000; Cavazos *et al*., 2002; Hewitson and Crane, 2002). Most automatic synoptic classifications or weather typing procedures use conventional statistical methods based on correlation fields or parametric clustering algorithms (Yarnal, 1993; Yarnal *et al*., 2001). These methods require that input data fit particular distributional assumptions and produce results that are often insensitive to inherent nonlinearities within the data sets. The SOM algorithm is able to discern nonlinear relationships within input data sets and does not require that the data fit any particular frequency distribution. It is an iterative algorithm that 'learns' the patterns of the input data vectors and organizes them into nodes within the SOM space (Hewitson and Crane, 2002). In developing a self-organized map, the user determines the dimensionality of the SOM space (i.e. number of 'clusters') prior to the classification. For example, a 4 by 3 node map would produce a map with 12 different weather types. These 12 'reference nodes' are initially seeded with random data vectors. The SOM algorithm examines input data vectors iteratively with respect to the reference nodes and assigns the input vector to the closest matching reference node. This 'winning' reference node is updated to resemble the input vector. The surrounding nodes are also updated to resemble the input vector, but with a much lower weighting. Iteratively updating the reference nodes and surrounding nodes through a neighborhood function eventually produces a spatially organized representation of the key weather types that span the continuum of

types in the input data set. This organization ensures that like patterns are in neighboring nodes and the most unlike patterns are in nodes farthest from each other along one of the diagonals of the SOM. This develops a continuum of types rather than discrete classes, which is particularly useful in examining daily transitions between weather types (Hewitson and Crane, 2002).

The SOM-based classification developed for this study used a 4×3 SOM to develop a 12-weather-type classification using daily 18Z 700-mb geopotential heights. The SOM algorithm used in the classification procedure was found in the SOM_PAK software package (Kohonen *et al*., 1995). The gridded daily data were from the Reanalysis data set produced by the National Centers for Environmental Prediction (NCEP) and National Center for Atmospheric Research (NCAR) (Kalnay *et al*., 1996). The Reanalysis data represent model reconstructions of various atmospheric fields from daily observations at a grid resolution of 2.5°. These data provide a spatially and temporally consistent global data set and are widely used in all types of climatological studies. The global data set was clipped to a 7×7 grid-point window centered over the southwest United States (Figure 1). The 700-mb level was used because of its proximity to the higher elevation areas of the Southwest. This level is higher than most Southwest topographic features for most of the year, but still low enough to be connected to surface weather regimes. The use of geopotential heights allows for both the examination of changes in surface temperatures and gradients that may control surface wind regimes. The 18Z Reanalysis time period was chosen to match up with the afternoon peak in extreme fire-weather conditions.

A 4×3 SOM was chosen as the optimal classification size because of its ability to identify a diversity of patterns without overgeneralizing. This was determined by producing a 2×3 classification and a 7×5 classification. The 7×5 SOM produced a very similar classification in pattern to the 4×3 classification with

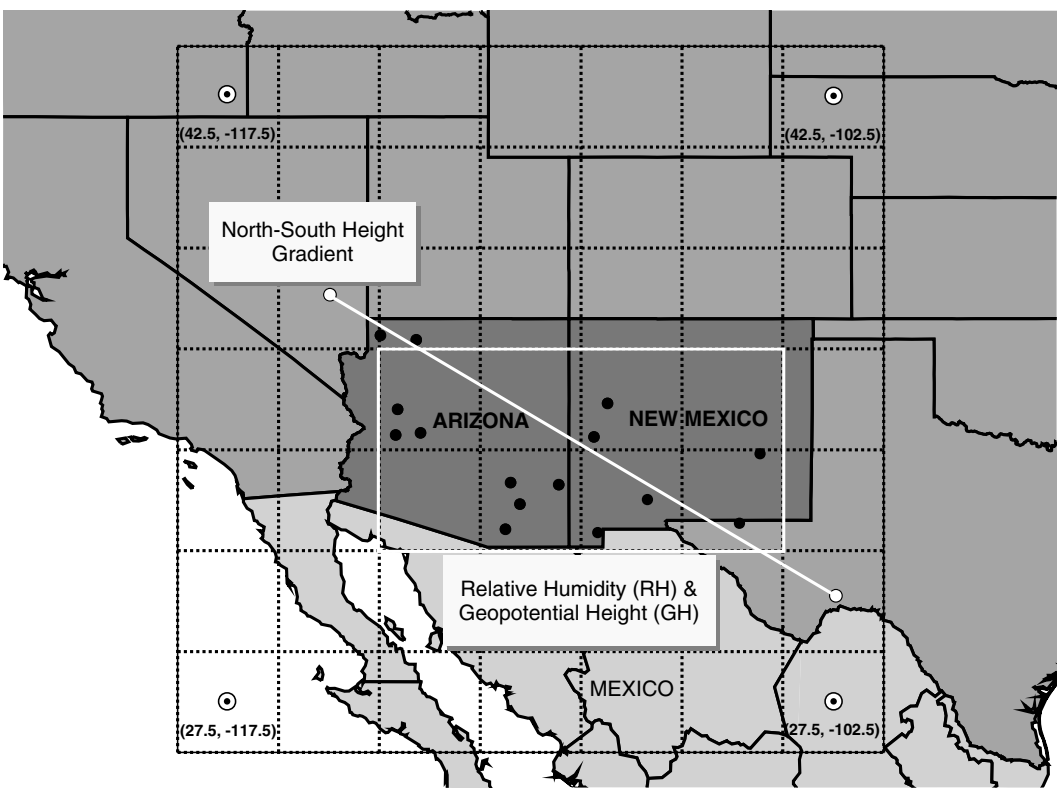

Figure 1. Study area showing location of RAWS sites (black dots) and NCEP–NCAR Reanalysis grid cells used in SOM classification. The diagonal white line represents transect along which geopotential height gradients were calculated and the white box highlights the eight grid cells used in calculation of average 700-mb relative humidity values (RH) and geopotential heights (GH). Reanalysis data grid points are located in the center of each grid cell (latitude and longitude shown for corner grid points)

a slightly higher level of detail. On the other hand, the 2×3 classification eliminated several patterns and appeared to be too general when compared with the patterns in the 4×3 and 7×5 SOMs. Parsimony guided toward the selection of the 4×3 SOM. It appears to capture the key daily patterns for April, May, and June (1988–2003) within a relatively small and easily interpretable number of classes.

2.2. *Daily fire-weather index*

The study period length was dictated by the availability of the surface data used to calculate the daily fire danger ratings. Surface data used in this study included daily weather observations from 15 remote automated surface weather stations (RAWS) for April, May, and June for the period of 1988–2003 (Figure 1). RAWS are designed to measure fire-weather conditions in remote locations and are sited on south-facing slopes in exposed areas to increase their sensitivity to extreme meteorological conditions (NWCG, 2000). Initially, 33 stations from across Arizona and New Mexico were considered for inclusion in the study. Short periods of record and missing data forced the exclusion of 18 stations. The final 15 stations included in the study represent the best spatial coverage of stations for the longest period of time.

Daily fire danger levels were determined by calculating daily Fosberg Fire-Weather Index (FFWI) values for each of the 15 stations. This index is essentially a nonlinear filter that is extremely sensitive to changes in wind speed and relative humidity levels (Fosberg, 1978; Goodrick, 2002). High winds and low relative humidity values result in high FFWI values (Fosberg, 1978). The FFWI is very similar in structure to the NFDRS spread component with a fixed fuel model. The FFWI integrates the Rothermel (1972) rate of spread calculation and the Simard (1968) equilibrium moisture content calculation to gauge fire-weather conditions in a similar manner as the NFDRS spread component index. Time series of daily FFWI and SC (fuel model G) values were highly correlated ($r > 0.95$) for all 15 stations. The FFWI was used because of its higher sensitivity to fine fuel moisture changes and its simple calculation with basic meteorological data. A statistical study by Haines *et al.* (1983) found the FFWI to be a strong and significant predictor of wildfire activity when compared to historical records in the northeastern United States.

The daily FFWI values from the 15 RAWS sites were combined into a time series by first converting the individual station time series into z-scores (subtracted from mean and then divided by standard deviation) and then averaging them together. Converting each station time series to z-scores standardizes the data set and does not allow any one station to dominate the global average time series. It is understood that averaging the individual time series created a loss of information, but the regional signal was the desired component of the variability in daily fire danger. Subregional variability in daily fire danger does exist, but is not addressed in this study.

The single, regional time series of FFWI z-scores was converted to rank-percentiles with the highest values being the highest percentiles. The 90th percentile was chosen as the breakpoint to determine extreme fire-weather conditions. This is a common threshold used by the fire management community to identify extreme fire-weather conditions (Fosberg *et al.*, 1993; Schlobohm and Brain, 2002). Chi-square tests were used to evaluate whether significant relationships existed between days with certain weather types produced by the SOM and days with 90th percentile FFWI values. Days that have FFWI values that exceed the 90th percentile are classified as 'exceedance days' and examined as days with extreme fire weather. Three particularly large and destructive Arizona and New Mexico wildfires were then examined with respect to the springtime weather types.

3. RESULTS AND DISCUSSION

3.1. *Identifying critical fire-weather patterns*

Classification of the daily height patterns into discrete classes allows for a more detailed examination of the high-frequency variability that characterizes the transition from winter circulation patterns to summer circulation patterns. Especially important to this study is the examination of the occurrence of steep horizontal height gradient patterns that produce high wind events at the surface. The synoptic pattern classification

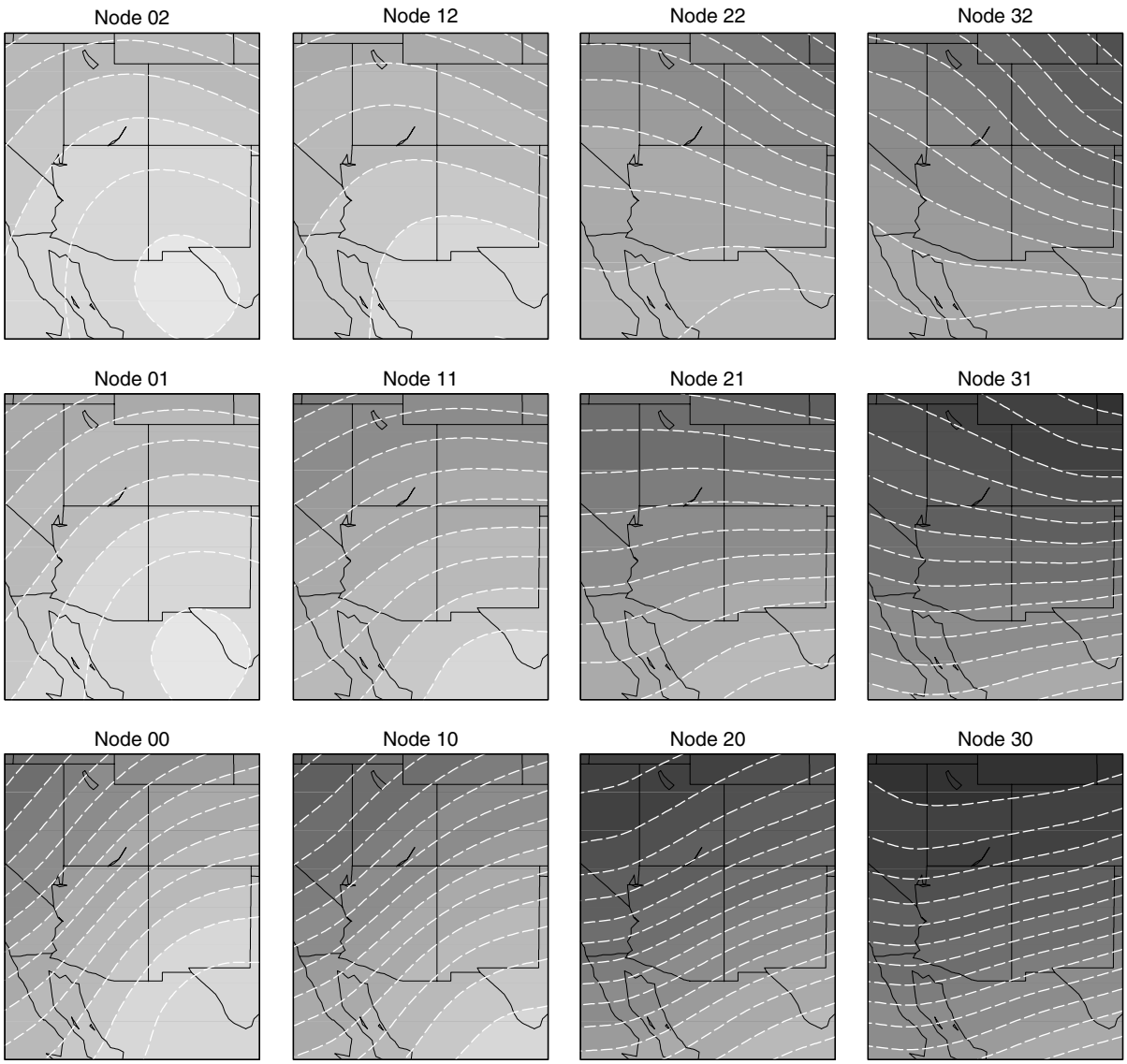

Figure 2. SOM classification of April–May–June daily gridded Reanalysis 18Z 700-mb geopotential heights for the period of 1988–2003. Highest height contour is in node 02 (3190 m) and lowest contour is in node 30 (3010 m). Contour interval is 10 m for all nodes

produced by the SOM algorithm is shown in Figure 2. This is a classification of all 700-mb geopotential height maps for each April, May, and June day for the period of 1988 through 2003 (1456 total days). Maximum class dissimilarity is oriented along the axis from node 02 (ridge pattern; weak height gradient) to node 30 (trough pattern; strong height gradient). The seasonal signal is evident in this synoptic classification, and is an important part of this analysis (Figure 3). The combined AMJ classification allows for consideration of all seasonal circulation patterns at once and to evaluate how these patterns evolve temporally. The lower-height patterns in the lower-right quadrant of the SOM are naturally more frequent in April, while the higher-height patterns in the upper-left quadrant are more often associated with June days. The sequence of daily weather types through a season in any given year of the study period is actually highly variable with a mixture of typical early season patterns occasionally occurring in June and late season patterns occurring in April. The occurrence of early season patterns (steep north–south height gradients) in May and June are of

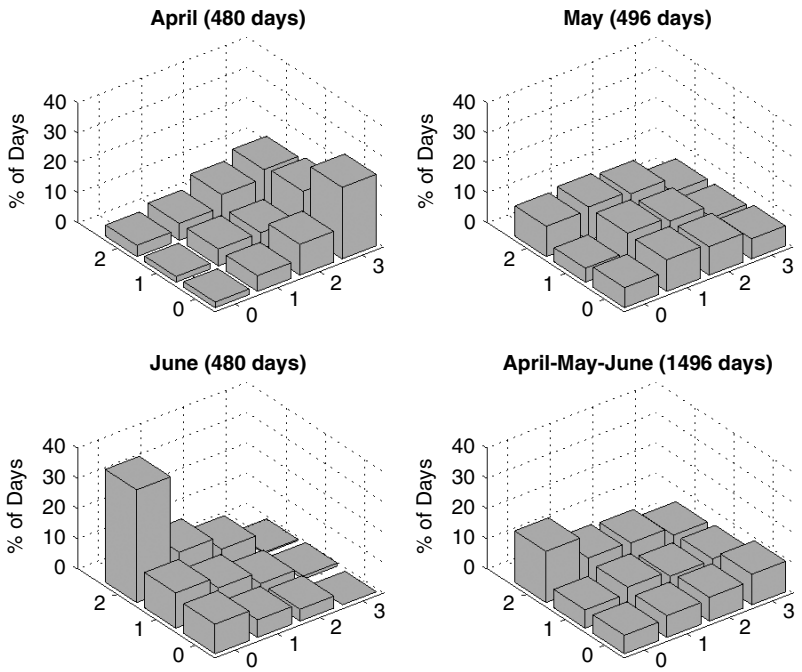

Figure 3. Frequency of occurrence of different SOM classified weather types. Organization of nodes is identical to that in Figure 2

Table I. Results of Chi-square tests between observed and expected FFWI 90th percentile exceedance counts associated with each weather type. Expected exceedance counts based on 10% of days within each weather type being associated with a 90th percentile exceedance by chance alone

	Node 02	Node 12	Node 22	Node 32
Total days	247	136	130	89
Observed	0	0	1	0
Expected	24.7	13.6	13	8.9
χ^2 p-value	<0.001	<0.001	<0.001	<0.001
	Node 01	Node 11	Node 21	Node 31
Total days	88	119	93	98
Observed	1	4	10	5
Expected	8.8	11.9	9.3	9.8
χ^2 p-value	0.009	0.024	1	0.147
	Node 00	Node 10	Node 20	Node 30
Total days	89	105	115	147
Observed	8	23	44	45
Expected	8.9	10.5	11.5	14.7
χ^2 p-value	0.888	<0.001	<0.001	<0.001

particular interest to this study because of their efficiency in producing high surface wind events during the arid foresummer that strongly influence wildfire behavior and spread.

The number of 90th percentile exceedance days associated with each weather type is shown in Table I. Expected frequencies representing no association between the number of exceedance days and each weather

type were calculated on the basis of 10% of days within each type producing an exceedance. Chi-square tests between observed and expected exceedance counts within each type show that nodes 10, 20, and 30 have significantly ($p < 0.001$) more exceedance days than would be expected by chance alone. Nodes 00, 21, and 31 have observed and expected frequencies that are not significantly different, while the remaining nodes all have significantly ($p < 0.05$) less exceedance days than should be expected. Node 02 has the largest membership of any node with 247 days (17% of total days), and not one exceedance day is associated with this weather type. Over 80% of the total number of exceedance days are associated with either node 10, 20, or 30. This finding indicates that these are important circulation patterns that elevate fire-weather conditions to extreme levels over the entire southwest United States simultaneously. These patterns are consistent with the findings of Schroeder (1969). His study identified a longwave trough–ridge pattern over the western United States that produced a southwest flow at upper levels (500 mb) as a critical fire-weather pattern for the southwest US region.

Nodes 10, 20, and 30 all reflect this general pattern, but with subtle differences in mean geopotential heights across the region, trough and ridge positions, and gradient intensity. Lowest geopotential heights are found in node 30 with increasing heights toward node 10 along the bottom row of the SOM classification. The pattern shift from node 30 to node 10 shows a retreating of the mean trough over the western United States toward the northwest and a ridge building from the southeast. These results identify a higher level of detail in critical fire-weather patterns for the southwest United States than previously identified by Schroeder (1969).

3.2. Seasonality of critical fire-weather patterns

Examination of the seasonal occurrence of nodes 10, 20, and 30 in Figure 3 shows that node 30 is primarily an April pattern, while nodes 10 and 20 occur throughout April, May, and June. The relationship between these circulation patterns and the occurrence of extreme fire-weather conditions changes throughout the AMJ season. Node 30 is both, the most frequent critical fire-weather pattern and the one associated with the most April exceedance days (Table II). Twenty-seven percent of node-20 days were associated with exceedance days compared to 25% for node 30. The occurrence of node-10 days was infrequent and was associated with an expected small number of exceedance days (Table II).

Typical Southwest springtime circulation patterns reflect increasing sun angles and increasing heights to the south. A strong baroclinic zone across Arizona and New Mexico is gradually displaced from the southeast by a subtropical ridge with weaker height gradients. The strong baroclinic zone is typically an early season (April) phenomena that dissipates through May and is virtually absent during June. This is evident in the gradual decrease through May and June in frequency of nodes 10, 20, and 30. Extreme FFWI values do not

Table II. Efficiency of critical fire-weather types at producing FFWI 90th percentile exceedances by month (Exc. days = exceedance days)

		Node 10	Node 20	Node 30	Combined
April	Total days	25	49	114	188
	Exc. days	2	13	28	43
	Efficiency	0.08	0.27	0.25	0.23
May	Total days	52	47	33	132
	Exc. days	9	21	17	47
	Efficiency	0.17	0.45	0.52	0.36
June	Total days	28	19	0	47
	Exc. days	12	10	0	22
	Efficiency	0.43	0.53	NA	0.47
Total	Total days	105	115	147	367
	Exc. days	23	44	45	112
	Efficiency	0.23	0.38	0.31	0.31

follow this same seasonal trend. The number of 90th percentile exceedance days linked to the critical weather types actually increases from April (43) to May (47) and then decreases into June (Table II). The actual efficiency (ratio of exceedance days associated with weather type to the total number of weather type days) of the relationship between exceedance days and the critical weather types increases to a maximum in June (0.47), indicating that 47% of all days classified to either nodes 10 or 20 are also 90th percentile exceedance days. Even though the occurrence of circulation patterns represented by nodes 10 and 20 are rather infrequent during June, they are critically important because of their efficiency in producing region-wide extreme fire-weather conditions. May stands out as having a relatively high efficiency ratio with all three critical weather types and the highest overall frequency of exceedance day events. May is a critical fire-weather month with respect to wind events because of this higher frequency of exceedance days.

3.3. Meteorological characteristics of critical fire-weather pattern days

The changing efficiency ratios between different nodes and different months appear to be related to seasonal changes in the cooccurrence of low surface relative humidity values and high wind speeds. Average monthly 700-mb relative humidity values drop across the region from 34.9% in April to 31.7% in June (Table III). The transition to circulation patterns that limit moisture advection into the region combined with increasing geopotential heights causes mean relative humidity values to drop through the spring season (Burnett, 1994; Sheppard *et al*., 2002). The overall mean horizontal geopotential height gradient responsible for regional-scale surface wind regimes is relatively high in April (42.1 m/1000 km) and May (42.8 m/1000 km), but decreases sharply in June (32.3 m/1000 km), with the subtropical ridge beginning to dominate the region.

The relative humidity and geopotential height gradient values associated with the critical fire-weather types deviate quite strongly from the average monthly values, helping to explain their association with extreme fire-weather conditions. Monthly average height gradient values for each of the critical fire-weather types are above their respective monthly averages, indicating that the pattern represents above-average surface wind conditions. Relative humidity values are also generally above the monthly means for nonexceedance days, indicating that these patterns are generally more humid than other circulation patterns occurring during the month. This is especially true for node 30 in April and May. Average relative humidity values are significantly lower on exceedance days relative to nonexceedance days. Node 30 has the highest relative humidity values for nonexceedance days and is most frequent during the beginning of the circulation pattern transition from

Table III. Average atmospheric properties for exceedance days and nonexceedance days associated with critical weather types. Nonexceedance day values are shown with exceedance day values in parentheses. All values were calculated from daily 18Z Reanalysis grid-point values (locations shown on Figure 1)

		Node 10	Node 20	Node 30	All Days
April	GH (m)	3134 (3140)	3096 (3140)	3033 (3048)[a]	3098
	RH (%)	29.1 (19.6)	37.1 (28.1)	45.1 (34.5)[b]	34.9
	Grad (m/1000 km)	67.7 (91.6)	80.6 (97.5)[a]	73.1 (93.2)[a]	42.1
	Days	23 (2)	36 (19)	86 (28)	480
May	GH (m)	3133 (3133)	3091 (3098)	3047 (3050)	3131
	RH (%)	27.1 (25.5)	33.6 (24.8)[b]	39.4 (29.7)[a]	33
	Grad (m/1000 km)	70.8 (109.1)[b]	78.7 (99.5)[b]	77.9 (90.7)	42.8
	Days	43 (9)	26 (21)	16 (17)	496
June	GH (m)	3130 (3134)	3092 (3099)	NA	3169
	RH (%)	32.6 (26.7)	33.7 (29.9)	–	31.7
	Grad (m/1000 km)	71.3 (84.5)	74.9 (107.4)[a]	–	32.3
	Days	16 (12)	9 (10)	–	480

GH: geopotential height, RH: relative humidity, Grad: geopotential height gradient ([a] $p < 0.05$. [b] $p < 0.01$. Exceedance (Vs) nonexceedance day values are significantly different)

winter into spring. The lower heights and connection to late season winter moisture sources make this the 'wettest' of the critical fire-weather types. This is especially evident during April when nonexceedance days have an average relative humidity of over 45%, while exceedance days have an average relative humidity of 34.5%.

Critical weather types are very frequent during April, but relative humidity values associated with these types are often too high to produce extreme surface fire-weather conditions. Average relative humidities drop and mean height gradients increase as the season progresses into May. The overall frequency of critical weather types decreases, but the ratio of exceedance days to total days increases with the convergence of these optimal fire-weather conditions. Node-30 nonexceedance days bring the highest relative humidities to the region, but occur much less frequently compared to April. More May-node-30 days have relative humidity values and height gradients sufficient to produce FFWI 90th percentile exceedances. Daily circulation patterns markedly shift toward node-10 and -20 days. Exceedance days associated with these patterns have much lower relative humidities and much higher height gradients than the average of all May days.

The critical fire-weather patterns occur much less frequently during June as compared to May and April, but have the highest association with exceedance days when they do occur (Table II). Only nodes 10 and 20 occur during June with a frequency of 22 days out of 480 June days classified in this study. The high ratio of exceedance days to nonexceedance days (Table II) associated with nodes 10 and 20 in June (0.47) could be attributed to June having the lowest average relative humidity (Table III: 31.7%) when compared with April (34.9%) and May (31.7%). Relative humidity values actually increase in June for nodes 10 and 20 for both exceedance and nonexceedance days. This is most likely associated with early season monsoon moisture seeping into the region from the southeast. Regardless, the humidity levels are low enough to efficiently produce extreme fire-weather conditions when coupled with high wind events. The ratio of exceedance days to nonexceedance days (0.53) found in node 20 in June (Table II) appears to be related to the extremely high height gradients consistently associated with exceedance days. The ten node-20 exceedance days in June produced a mean height gradient of 107.4 m/1000 km compared to the June average of 32.3 m/1000 km (Table III). Node 10 (June) also has a relatively high ratio of exceedance to nonexceedance days that may be more a function of the combined effect of low relative humidity values and a relatively high height gradient even though exceedance day values are not significantly different from nonexceedance days (Table III).

3.4. Synoptic climate and wildfire events

It is difficult to determine the importance of extreme fire-weather conditions in producing large fire events when examining raw seasonal fire statistics or even daily fire records. Most long-term fire records do not contain information on the daily progression of individual wildfire events. Wildfires can burn for weeks, but may accumulate most of their total area burned during only a few days associated with extreme fire-weather conditions. Three case studies are used to examine the relationship between daily fire progression, critical fire-weather types, and weather type transitions.

Two of the three case study wildfires examined include the Aspen wildfire of June 2003 in southern Arizona and the Cerro Grande wildfire of May 2000 in northern New Mexico. An examination of the weather types and daily fire activity for each of the wildfires reveals that active fire days (large changes in area burned) were associated with the critical fire-weather types identified in this study. The Aspen fire in southern Arizona interacted with the critical fire-weather circulation patterns during its first week of burning in June of 2003. The synoptic circulation over the southwest United States transitioned from the more typical June, ridge-dominated pattern of node 02 to the high height gradient patterns of nodes 10 and 20 (Figure 4). Extreme fire-weather conditions persisted for more than a week with these patterns dominating the entire Southwest. The fire was especially active on June 23, burning more than 8500 acres in one day (Arizona Daily Star, 2003). Calmer winds returned when conditions transitioned back to the ridge-dominated pattern of node 02 on June 26. The fire continued to progress for several more weeks and burned a total of 82 000 acres.

The Cerro Grande wildfire of 2000, a major Southwestern wildfire event that threatened the Los Alamos National Laboratory, similarly transitioned from low-fire activity to extreme rates of growth when encountering the critical fire-weather types. It was a prescribed fire that escaped on May 5 eventually consuming more

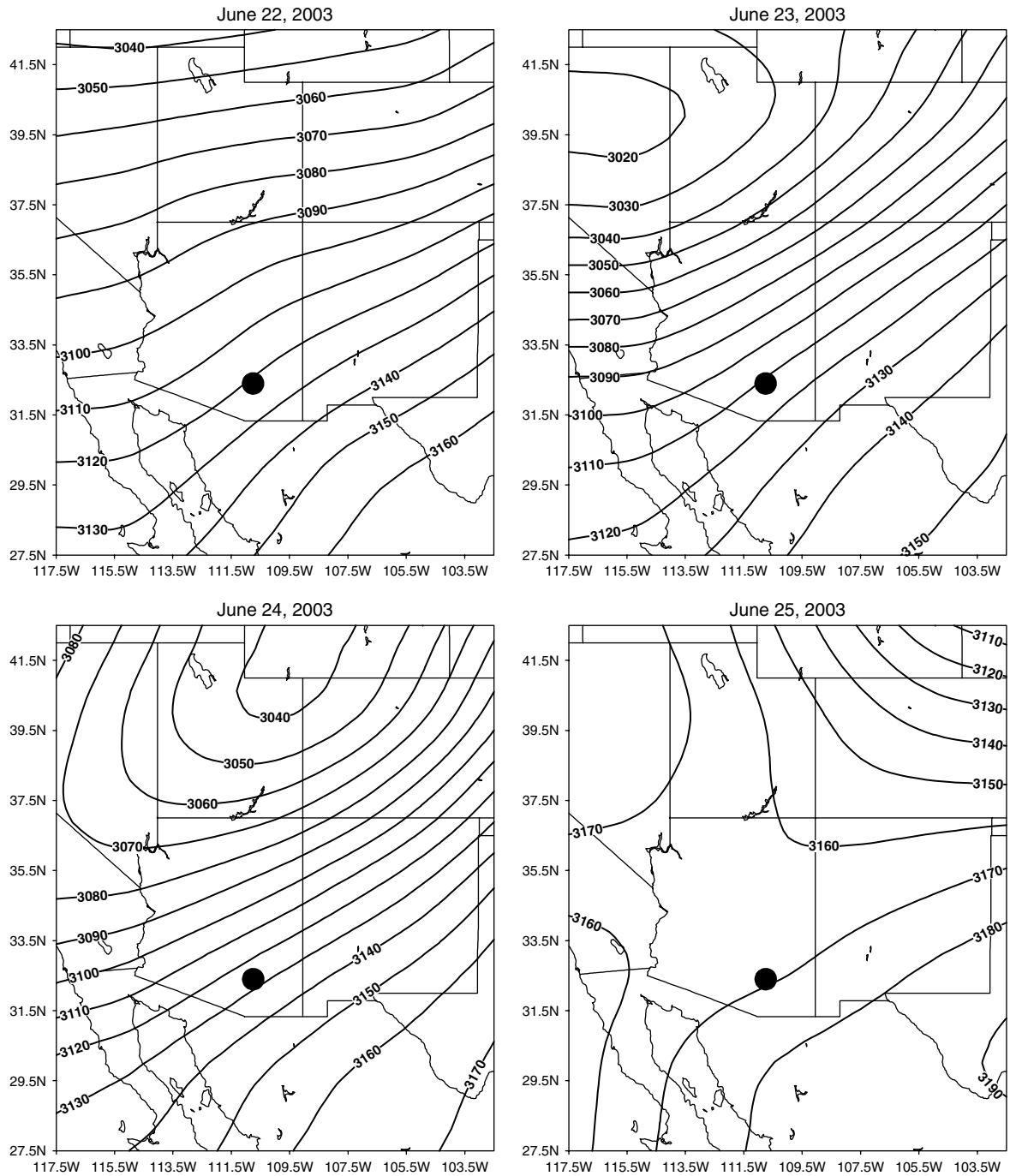

Figure 4. Daily (18Z) 700-mb geopotential height plots of Reanalysis data for a four-day period during the Aspen wildfire (closed circle) in southern Arizona in June of 2003. The wildfire was especially active on June 23, burning more than 8500 acres in one day

than 43 000 acres and destroying more than 400 homes in Los Alamos, New Mexico. A weaker gradient circulation pattern (node 11) was present on May 4, the initial day of the prescribed burn. The transition to a steeper gradient pattern (node 10) on May 5 brought higher winds to northern New Mexico causing the fire to

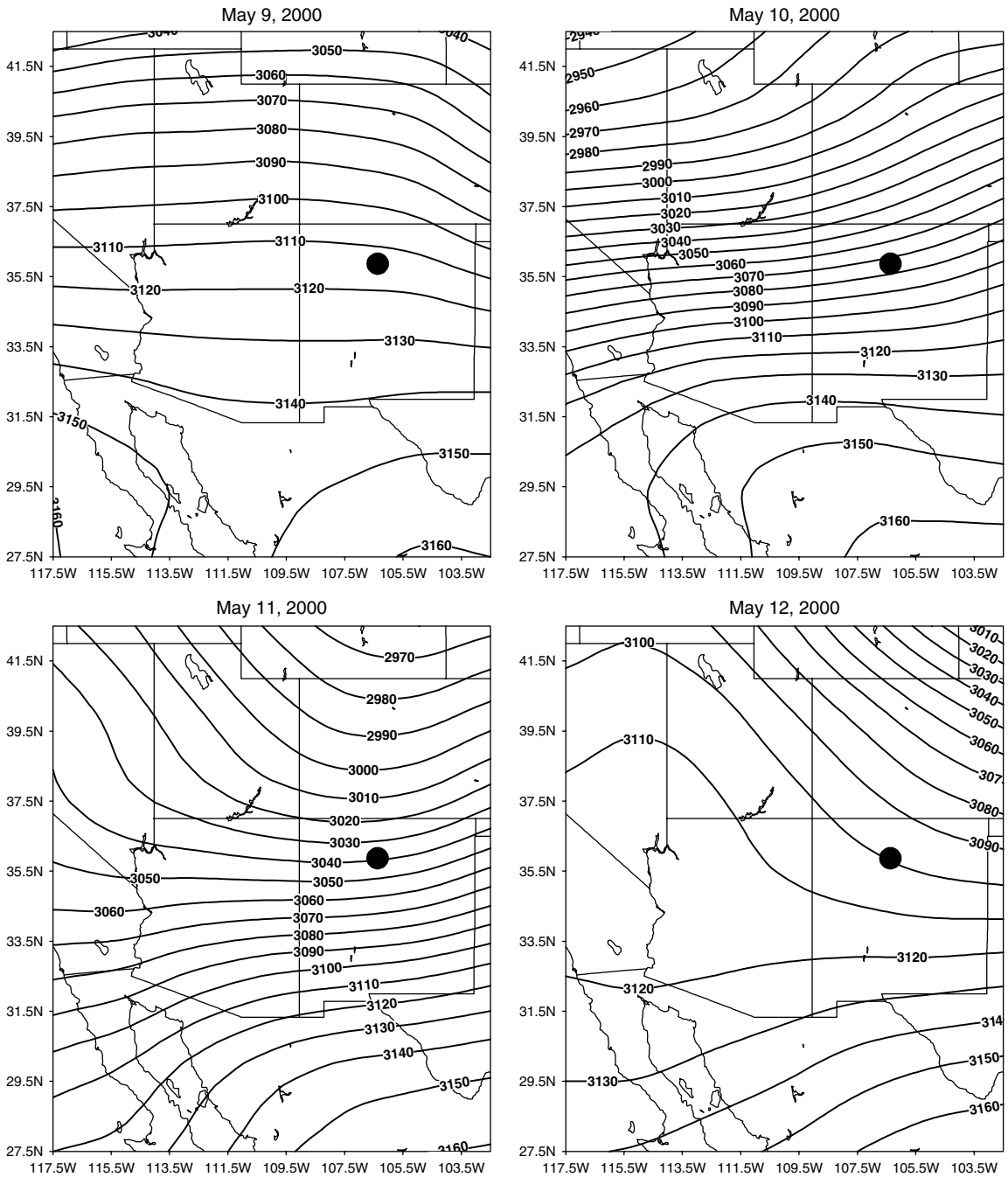

Figure 5. Daily (18Z) 700-mb geopotential height plots of Reanalysis data for a four-day period during the Cerro Grande wildfire (closed circle) in northern New Mexico in May of 2000. May 10 and 11 were the most active days of the Cerro Grande event with over 8000 acres burning on the 10th and 19 000 acres on the 11th

escape prescription. Height gradients continued to increase over the next several days with a deepening west coast trough (Figure 5). This was reflected in the synoptic classification with days transitioning from node 10 to node 20 on May 10. The occurrence of a node-20 circulation pattern on May 10 brought extremely high winds, causing the fire to grow in size dramatically and burn over 8000 acres in one day (Table IV).

Table IV. Progression of Cerro Grande wildfire and synoptic weather types. Adjusted transition probabilities were calculated by removing the transitions that occurred during the period of May 2, 2000 through May 15, 2000. The Jemez, NM RAWS is located 20 miles west of Los Alamos, NM

Date	Synoptic weather type	Acres burned/day	Adjusted transition probability	Frequency of transition occurrence: 1988–2003	Jemez, NM RAWS Data		
					Ave. temp (°F)	Ave. relative humidity (%)	Max. wind gust (mph)
5/2/00	22	*Prefire*			53	34	27
5/3/00	11	*Prefire*	15.7	8	60	16	34
5/4/00	11	*Prescription*	19.6	10	62	13	23
5/5/00	10	*Declared Wildfire*	18	9	63	10	31
5/6/00	10	805	20	10	60	12	37
5/7/00	21	1553	18.2	8	61	19	33
5/8/00	21	857	18.2	8	55	31	39
5/9/00	21	660	18.2	8	57	23	27
5/10/00	20	8127	13	6	63	20	37
5/11/00	30	19 542	31.3	10	58	19	42
5/12/00	32	2852	16	4	42	12	28
5/13/00	11	6300	3.92	2	48	21	22
5/14/00	00	1563	9.68	9	55	23	23
5/15/00	00	414	32.3	10	Missing	Missing	33

3.5. Synoptic circulation patterns and the Cerro Grande fire

Examination of the sequence of synoptic types prior to and during the Cerro Grande wildfire can help explain if these weather conditions were extraordinary for May in the southwest United States. A shortwave trough had just exited the region the previous week, leading to a transition pattern classification (node 22) on May 2, two days prior to the prescribed fire at Cerro Grande (Table IV and Figure 6). Transition probabilities between all synoptic weather types were calculated to determine the preferential sequences of weather types that occur during May (Table V). These probabilities were calculated by dividing the transition frequency (between two weather types) by the overall frequency of the base weather type. The node-22 weather type on May 2 not only had the highest probability of persisting for another day based on the 1988–2003 record but also had a relatively high probability of transitioning into a ridge pattern found in either node 11 or node 12. Ridging behind a departing shortwave is common, but the transition to node 11 instead of 12 indicates that the ridging was not very strong and that subsequent days would experience circulation patterns with increasing geopotential height gradients across the region (weak ridging).

The node-11 circulation pattern persisted for another day, but had almost equal chances of transitioning into a weaker-gradient ridge pattern (node 01) or having the height gradient strengthen with the pattern in node 10. The establishment of the node 10 patterns shifts the subsequent probabilities away from quickly returning to strong ridging and weaker height gradients found in the upper-left-hand corner of the SOM classification. Once in node 10 (May 6), the highest probability transition is to a deepening trough pattern to the west (node 20) or to have the ridge flatten (node 21).

The ridge flattened on May 7 (node 21) and persisted for three days, bringing cooler temperatures and lighter winds. The total acres burned per day reflect the calmer conditions experienced on these days. An important transition occurred from May 9–10, when the circulation moved toward the critical fire-weather pattern of node 20. The highest probability transitions from node 21 were along the diagonal axis of the SOM, with a 15.9% chance of transition to node 32 and an 18.2% chance of transition to node 10. The highest probability transition on a node-21 day, besides persistence, is the transition toward the critical fire-weather pattern of node 10. The lower probability (13.6%) actual transition to node 20 had the same effect of dramatically increasing the geopotential height gradient across the region and increasing surface winds.

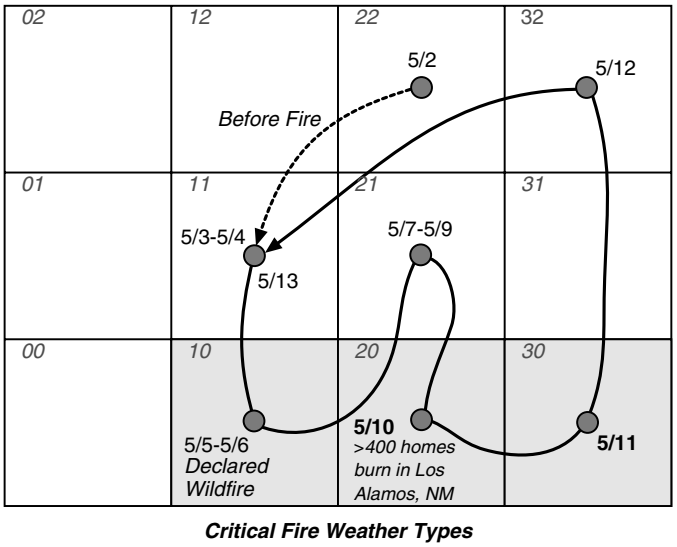

Figure 6. Sequence of daily weather types prior to and through the first week of the Cerro Grande wildfire. Dates in bold indicate most active fire days

Table V. Transition frequencies and probabilities for all May days, 1988–2003. First number in each cell is transition probability (%) and second number is frequency of occurrence (days)

Day 1 \ Day 2	00	01	02	10	11	12	20	21	22	30	31	32	Total Days
00	34.4 11	9.4 3	3.1 1	28.1 9	12.5 4	3.1 1	3.1 1	6.3 2	0 0	0 0	0 0	0 0	32
01	18.2 4	22.7 5	18.2 4	9.1 2	18.2 4	13.6 3	0 0	0 0	0 0	0 0	0 0	0 0	22
02	6.4 3	10.6 5	51.1 24	0 0	2.1 1	27.7 13	0 0	0 0	2.1 1	0 0	0 0	0 0	47
10	9.6 5	1.9 1	0 0	21.2 11	9.6 5	0 0	25.0 13	17.3 9	5.8 3	7.7 4	0 0	1.9 1	52
11	8.0 4	8.0 4	6.0 3	20.0 10	22.0 11	10.0 5	4.0 2	6.0 3	16.0 8	0 0	0 0	0 0	50
12	5.6 3	7.4 4	24.1 13	1.9 1	13.0 7	27.8 15	0 0	0 0	20.4 11	0 0	0 0	0 0	54
20	0 0	0 0	0 0	6.3 3	0 0	2.1 1	29.2 14	12.5 6	4.2 2	22.9 11	16.7 8	6.3 3	48
21	2.1 1	2.1 1	0 0	19.1 9	19.1 9	0 0	14.9 7	21.3 10	6.4 3	2.1 1	6.4 3	6.4 3	47
22	3.7 2	0 0	9.3 5	5.6 3	16.7 9	24.1 13	3.7 2	5.6 3	22.2 12	1.9 1	1.9 1	5.6 3	54
30	0 0	0 0	0 0	2.9 1	0 0	0 0	8.6 3	5.7 2	0 0	37.1 13	31.4 11	14.3 5	35
31	0 0	0 0	0 0	3.8 1	3.8 1	3.8 1	11.5 3	19.2 5	15.4 4	7.7 2	11.5 3	23.1 6	26
32	0 0	0 0	0 0	6.9 2	10.3 3	10.3 3	6.9 2	24.1 7	20.7 6	3.4 1	0 0	17.2 5	29

Over 8000 acres burned on May 10 with the increase in wind speeds, including over 400 homes in the town of Los Alamos (NPS, 2001). The transition to node 30 on the 11th brought even higher winds to the area, pushing the fire onto the grounds of the Los Alamos National Laboratory and consuming almost 20 000 acres in one day. A relatively unusual and fortunate change in circulation occurred from May 11–12.

The deep western trough on May 11 (node 30) moved to the east on May 12, bringing a weaker gradient and calmer winds (node 32) to northern New Mexico. Of the 33 days in this study classified as a node-30 pattern, a one-day transition to a node-32 circulation pattern has only occurred twice. The more frequent node-30 transitions include persistence or a rebuilding of the ridge to the south (node 20); both produce continued high surface winds. Total area burned per day was substantially less over the next several days as gradients weakened slightly with circulation patterns transitioning back toward the prefire conditions of node 11 and node 00 (Figure 6).

The transition probabilities were calculated for May alone, which reduced the overall sample size and robustness of the probability values. This was necessary because transition probabilities would be very different between June patterns and April patterns. Days would be biased toward lower-height days in April and higher-height days in June because of the normal increase in geopotential heights over the region through the spring season. The May transition probabilities need to be interpreted with care because of the very low number of transitions in some node combinations. Regardless, the probabilities allow for a diagnosis of preferential transitions and level of persistence in comparison to actual events and may be useful in operational fire-weather forecasting.

3.6. Large wildfires and noncritical fire-weather types

The three critical fire-weather circulation patterns in this study (nodes 10, 20, and 30) are related to elevated fire danger because they produce both high surface wind speeds and low relative humidity values. These meteorological conditions can produce high rates of spread during wildfire events, hampering suppression efforts and quickly pushing fires to large sizes. These conditions are not always directly related to the larger-scale synoptic circulation. The third case study wildfire is used to illustrate this point. The central Arizona Rodeo-Chediski wildfire in June 2002 burned over 460 000 acres in less than four weeks (Schoennagel *et al.*, 2004). Ten of the first 13 days of the wildfire event were classified to the node 02 circulation pattern, which represents strong ridging (Figure 2). Wilmes *et al.* (2002) determined that the combination of exceptionally dry fuels from the Southwestern drought, topography, and the development of plume-driven fire dynamics drove the extreme fire behavior experienced during the duration of the Rodeo-Chediski fire. A plume-dominated wildfire will periodically develop a large convective cloud of ash and hot gases that cools and collapses back into the center of fire activity. This collapse produces extreme surface winds and can drive high rates of spread (Pyne *et al.*, 1996). The meteorological conditions important to this Rodeo-Chediski wildfire were more local scale and related to atmospheric stability than to larger-scale synoptic flow patterns. More work will be done to assess the average atmospheric stability associated with each weather type in this study.

4. CONCLUSIONS

The SOM synoptic classification produced three weather types that were consistently related to extreme surface fire-weather conditions. Over 80% of extreme (>90th percentile), regional FFWI values are associated with the weather types represented in nodes 10, 20, and 30. These patterns represent circulation patterns of high gradient, southwest flow across the southwest United States and are very similar to the critical fire-weather pattern identified by Schroeder (1969). The three weather types identified in this study are different seasonal representations of the broadly defined Schroeder 'southwest flow' pattern. The intensity of the height gradient, average relative humidity values, and average geopotential height change from month to month in response to seasonal changes for each of the critical fire-weather types. The characteristics between exceedance days and nonexceedance days also change through the season with the greatest differences occurring with nodes 20 and 30 in April and May. Early season variability in relative humidity levels appears to be a factor that controls the level of FFWI values associated with node 30 days.

The occurrence of critical fire-weather types decreases through the season from April into June. May has the most efficient relationship between the occurrence of exceedance days and critical weather fire-weather types. High geopotential height gradients and low relative humidity values characterize exceedance days that

occur with nodes 10, 20, or 30. Ridging from the expansion of the subtropical high dominates most days by the end of May into June. Critical fire-weather types are very infrequent in June, but do occasionally occur. About 50% of the node-10 and -20 days that occur in June are also exceedance days.

The critical fire-weather patterns identified in this study have proven to be important to recent catastrophic wildfire events. Strong winds with the node 10, 20, and 30 weather types caused the Cerro Grande fire to burn more than 400 homes in Los Alamos, New Mexico. It is difficult to determine how often wildfire events interact with these critical circulation patterns. Long-term records of wildfire statistics typically do not provide daily progression summaries for the duration of wildfire events. Only recently have wildfires been documented in this way, limiting the present analysis to case studies. The identification of the climatology of these patterns may have utility in the planning capacity for prescribed burning activities. When used with weather forecasts prior to a prescribed burn, they can help elucidate possible changes in fire-weather conditions with respect to large-scale circulation features during the burn period.

Characterizing the interannual variability in the frequency of these weather types may help explain some of the variance in seasonal wildfire activity. These critical weather types are nested within the global atmospheric circulation and may be subject to preferential modes of variability and part of low-frequency teleconnection patterns. Identification of these critical patterns allows for further analysis into connections between global climate variability and regional wildfire variability. Further work could identify changes in the frequency of these weather types in general circulation model predictions to assess how regional fire-weather conditions may change under different climate regimes. The connections between high- and low-frequency climatic variability are an important, but poorly understood, component of overall wildfire-climate interactions.

ACKNOWLEDGEMENTS

This research was funded in part by a Space Grant Graduate Fellowship. The author wishes to thank to Beth Hall and Hauss Reinbold for the great amount of assistance they provided in obtaining the RAWS data critical for this study. David McGinnis, Tereza Cavazos, and Bruce Hewitson helped provide sample code to process and visualize the results. Many thanks also to Theresa Mau-Crimmins, Andrew Comrie, Katie Hirschboeck, Thomas Swetnam, Tim Brown, and Gregg Garfin who all provided reviews that improved the final manuscript.

REFERENCES

Andrews PL, Queen LP. 2001. Fire modeling and information system technology. *International Journal of Wildland Fire* **10**: 343–352.

Arizona Daily Star. 2003. *Aspen Wildfire*, Arizona Daily Star: Lee Enterprises Inc Tucson, AZ. Available online http://www.azstarnet.com/wildfire/aspenfireindex.html, Accessed: August 2004.

Bessie WC, Johnson EA. 1995. The relative importance of fuels and weather on fire behavior in Sub-Alpine forests. *Ecology* **76**(3): 747–762.

Brotak EA, Reifsnyder WE. 1977. An investigation of the synoptic situations associated with major wildland fires. *Journal of Applied Meteorology* **16**: 867–870.

Burgan RE. 1988. *1988 Revisions to the 1978 National Fire Danger Rating System*, United States Forest Service SE-273, Asheville, NC.

Burgan RE, Andrews PL, Bradshaw LS, Chase CH, Hartford RA, Latham DJ. 1997. WFAS: Wildland fire assessment system. *Fire Management Notes* **57**(2): 14–17.

Burnett AW. 1994. Regional-Scale troughing over the Southwestern United States: Temporal climatology, teleconnections, and climatic impact. *Physical Geography* **15**(1): 80–98.

Cavazos T. 2000. Using Self-Organizing maps to investigate extreme climate events: an application to wintertime precipitation in the Balkans. *Journal of Climate* **13**: 1718–1732.

Cavazos T, Comrie AC, Liverman DM. 2002. Intraseasonal variability associated with Wet Monsoons in Southeast Arizona. *Journal of Climate* **15**: 2477–2490.

Crimmins MA, Comrie AC. 2004. Wildfire-Climate interactions across Southeast Arizona. *International Journal of Wildland Fire* **13**(4): 455–466.

Deeming J, Burgan RE, Cohen J. 1977. *The National Fire Danger Rating System – 1978*, United States Forest Service GTR-INT-39, Ogden, UT.

Flannigan MD, Harrington JB. 1988. A study of the relation of meteorological variables to monthly provincial area burned by wildfire in Canada (1953–80). *Journal of Applied Meteorology* **27**: 331–452.

Flannigan MD, Wotton BM. 2001. Climate, weather, and area burned. In *Forest Fires: Behavior and Ecological Effects*, Johnson EA, Miyanishi K (eds). Academic Press: San Deigo, CA, 351–373.

Fosberg MA. 1978. *Weather in Wildland Fire Management: The Fire Weather Index, Conference on Sierra Nevada Meteorology*. American Meteorological Society: Lake Tahoe, CA.
Fosberg MA, Mearns L, Price C. 1993. Climate change – fire interactions at the global scale: Predictions and limitations of methods. In *Fire in the Environment: The Ecological, Atmospheric, and Climatic Importance of Vegetation Fires*, Crutzen PJ, Goldammer JG (eds). John Wiley & Sons: Chicester.
Fujioka F. 1997. High resolution fire weather models. *Fire Management Notes* **57**: 22–25.
Goodrick SL. 2002. Modification of the Fosberg fire weather index to include drought. *International Journal of Wildland Fire* **11**: 205–211.
Haines DA, Main WA, Frost JS, Simard AJ. 1983. Fire-danger rating and wildfire occurrence in the Northeastern United States. *Forest Science* **29**(4): 679–696.
Hewitson BC, Crane RG. 2002. Self-organizing maps: applications to synoptic climatology. *Climate Research* **22**: 13–26.
Johnson EA, Wowchuk DR. 1993. Wildfires in the southern Canadian rocky mountains and their relationship to mid-tropospheric anomalies. *Canadian Journal of Forest Research* **23**: 1213–1222.
Kalnay E, Kanamitsu M, Kistler R, Collins W, Deaven D, Gandin L, Iredell M, Saha S, White G, Wallen J, Zhu Y, Leetmaa A, Reynolds B, Chelliah M, Ebisuzaki W, Higgins W, Janowiak J, Mo KC, Ropelewski, Wang J, Jenne R, Joseph D. 1996. The NCEP-NCAR 40-Year Reanalysis project. *Bulletin of the American Meteorological Society* **77**(77): 437–471.
Kohonen T. 2001. *Self-Organizing Maps*. Springer: New York, 501.
Kohonen T, Hynninen J, Kangas J, Laaksonen J. 1995. SOM_PAK: The self-organizing map package, v. 3.1. Helsinki Finland, Laboratory of Computer and Information Science, University of Helsinki.
NWCG. 2000. National Fire Danger Rating System: Weather Station Standards. Boise, National Wildfire Coordinating Group. PMS 426-3: 31.
NPS. 2001. *Cerro Grande Prescribed Fire: Board of Inquiry Final Report*, National Park Service: Sante Fe, New Mexico. 52.
Pyne SJ, Andrews PL, Laven RD. 1996. *Introduction to Wildland Fire: Fire Management in the United States*. Wiley: New York, 455.
Rothermel RC. 1972. *A Mathematical Model for Predicting Fire Spread in Wildland Fuels*, Intermountain Forest and Range Experiment Station Research Paper INT-115, Ogden, UT.
Schlobohm PM, Brain J. 2002. *Gaining an understanding of the National Fire Danger Rating System*. National Wildfire Coordinating Group: Boise, ID, 82.
Schoennagel T, Veblen TT, Romme WH. 2004. The interaction of fire, fuels, and climate across Rocky mountain forests. *BioScience* **54**(7): 661–676.
Schroeder MJ. 1969. *Critical Fire Weather Patterns in the Conterminous United States*. Environmental Science Services Administration: Silver Spring, MD.
Sheppard PR, Comrie AC, Packin GD, Angersbach K, Hughes MK. 2002. The climate of the U.S. Southwest. *Climate Research* **21**: 219–238.
Simard AJ. 1968. *The Moisture Content of Forest Fuels: A Review of the Basic Concepts*. Forest Fire Research Institute: Ottawa, Ontario.
Swetnam TW, Betancourt JL. 1990. Fire-Southern oscillation relations in the southwestern United States. *Science* **249**: 1017–1020.
Swetnam TW, Betancourt JL. 1998. Mesoscale disturbance and ecological response to decadal climatic variability in the American Southwest. *Journal of Climate* **11**: 3128–3147.
Takle ES, Bramer DJ, Heilman WE, Thompson MR. 1994. A synoptic climatology for forest fires in the NE US and future implications from GCM simulations. *International Journal of Wildland Fire* **4**: 217–224.
Westerling AL, Gershunov A, Cayan DR, Barnett TP. 2002. Long lead statistical forecasts of area burned in western U.S. wildfires by ecosystem province. *International Journal of Wildland Fire* **11**: 257–266.
Westerling AL, Brown TJ, Gershunov A, Cayan DR, Dettinger MD. 2003. Climate and Wildfire in the Western United States. *Bulletin of the American Meteorological Society* **84**(5): 595–604.
Wilmes L, Martinez D, Wadleigh L, Denton C, Geisler D. 2002. *Apache-Sitegreaves National Forests Rodeo-Chediski Fire Effects Summary Report*. Apache-Sitegreaves National Forest: Springerville, AZ.
Yarnal B. 1993. *Synoptic Climatology in Environmental Analysis*. Belhaven Press: London.
Yarnal B, Comrie AC, Frakes B, Brown DP. 2001. Developments and prospects in synoptic climatology. *International Journal of Climatology* **21**: 1923–1950.

